Interplay of Lyapunov exponents, phase transitions, and chaos bound in nonlinear electrodynamics black hole

Chuanhong Gao[1†] Chuang Yang (杨创)[2‡] Tetvui Chong[1§] Deyou Chen (陈德友)[2¶]

[1]Faculty of Engineering and Quantity Surveying, INTI International University, Nilai 71800, Malaysia
[2]School of Science, Xihua University, Chengdu 610039, China

Abstract: In this study, we investigate Lyapunov exponents of chaos for both massless and charged particles around a non-linear electrodynamics black hole and explore their relationships with a phase transition and chaos bound of this black hole. Our results indicate that these exponents can effectively reveal the phase transition. Specifically, during the phase transition, violation of the chaos bound occurs solely within a stable branch of a small black hole. Moreover, the violations are observed regardless of whether the phase transition takes place.

Keywords: Lyapunov exponent, phase transition, NLED black hole

DOI: 10.1088/1674-1137/ae210d **CSTR:** 32044.14.ChinesePhysicsC.50035101

I. INTRODUCTION

Phase transitions of black holes (BHs) have long attracted attention. The foundational work in this direction was initiated by Hawking and Page through their investigation of the Schwarzschild anti-de Sitter (AdS) spacetime [1]. They discovered the first-order phase transition between a large BH and a thermal AdS vacuum, known as the Hawking-Page phase transition. When the temperature is below the critical value, the thermal AdS vacuum phase is more stable; conversely, when the temperature exceeds the critical value, the BH phase dominates. The phase structure of AdS BHs is fascinating in the thermodynamic context of an extended phase space, where the cosmological constant is regarded as thermodynamic pressure [2, 3]. In [4], Kubiznak and Mann examined the thermodynamic properties of the Reissner-Nordström (RN) AdS BH within the framework of an extended phase space. It was found that this BH exhibits van der Waals-like phase transition behavior, with the P-V criticality matching the P-T diagram and the P-T coexistence line terminating at the phase transition point. Subsequently, in-depth studies have been conducted on the phase behavior and P-V criticality of other BHs within the extended phase space framework [5–7], and the critical exponents associated with phase transitions have been determined. These critical exponents are in perfect agreement with those of classical van der Waals fluids. For other interesting results on thermodynamic research in extended phase spaces, please refer to [8–23].

In recent years, the connections between BH phase transitions and observable physical quantities have been explored. For instance, the behaviors of physical quantities such as the circular orbit radius of test particles [24–26], the BH shadow [27, 28], and quasinormal modes (QNMs) [29–32] can reveal the phase structure of BHs. The discontinuous changes in these physical quantities near the phase transition point are analogous to the behavior of order parameters.

A Lyapunov exponent (LE) serves as an indicator to describe the rate of separation of adjacent trajectories in a dynamical system. A positive exponent value indicates that adjacent orbits diverge over time, signifying a chaotic system, whereas a negative exponent value implies that adjacent orbits converge over time, describing the stability of the motion of the system. This approach has been widely applied in the study of chaotic dynamics in general relativity [33–43]. It is not only used to identify the chaotic motion of particles in BH backgrounds, but is also closely related to fundamental issues such as BH area quantization and the determination of QNM frequencies. Notably, there is a close relationship between the exponent and imaginary part of QNMs [44], and the QNMs of BHs are associated with their phase transitions. Recent research has provided a new approach for using LEs to detect phase transitions [45]. In this work, the authors first investigated the relationship between the chaotic motion of particles around the RN AdS BH and its thermo-

Received 16 July 2025; Accepted 19 November 2025; Accepted manuscript online 20 November 2025

† E-mail: chuanhonggao@hotmail.com (Corresponding author)
‡ E-mail: chuangyangyc@hotmail.com
§ E-mail: chongtetvui@gmail.com
¶ E-mail: deyouchen@hotmail.com (Corresponding author)

dynamic phase transition. The study revealed that when the phase transition occurs, the exponent exhibits multi-valuedness, with its branches corresponding to the phase structure of this BH. Moreover, the discontinuous change in the exponent can be regarded as an order parameter that possesses a critical exponent of 1/2 near the critical point. Subsequent research has extended this work to other spherically symmetric spacetimes [46–52].

There are various methods for determining the exponent discussed in previous works [44, 53–56]. In this study, we adopt the method proposed by Lei and Ge [57, 58], which determines the exponent by calculating the eigenvalues of the Jacobian matrix. We investigate the LEs of both massless and charged particles orbiting a nonlinear electrodynamics (NLED) BH in the canonical ensemble and explore their relationships with the phase transitions of this BH and the chaos bound. As an extension of the Born-Infeld and Euler-Heisenberg electrodynamics, the NLED has garnered significant attention since its proposal. For example, this model can explain the early universe expansion [59]; certain NLED models can serve as alternatives to dark energy to describe the accelerated expansion of the universe and eliminate the Big Bang singularity [60]. The first regular BH solution of this model was obtained by Bardeen [61]. Subsequently, Bronnikov discovered a class of magnetically charged regular BHs within the framework of coupling general relativity with a specific model [62]. Hayward identified a specific model that can describe BH collapse and evaporation [63]. Balart and Vagenas derived multiple regular BH solutions with nonlinear electrodynamics [64], and Yu and Gao derived an exact solution for the RN BH with nonlinear electromagnetism [65]. For regular solutions derived from other NLED models, please refer to [66].

The remainder of this paper is organized as follows. In Section II, we first briefly review the thermodynamics of the NLED BH. In Section III, we calculate the LEs for both massless and charged particles orbiting the NLED BH and explore their relationship with the phase transition. In Section IV, we discuss the chaos bound in this BH. Section V presents our conclusions.

II. THERMODYNAMICS OF NLED BH

The minimal interaction between NLED theory and gravity is described as

$$S = \frac{1}{16\pi}\int \sqrt{-g}\,(R + K(\psi))\,\mathrm{d}^4x, \tag{1}$$

where

$$F_{\mu\nu} = \nabla_\mu A_\nu - \nabla_\nu A_\mu, \quad \psi = F_{\mu\nu}F^{\mu\nu}. \tag{2}$$

In the above equation, R represents the Ricci scalar, A_ν denotes the Maxwell field, and $K(\psi)$ is a nonlinear function of ψ. The corresponding field equations are obtained by varying the above action.

$$G_{\mu\nu} = \frac{1}{2}g_{\mu\nu}K[\psi] - 2K[\psi]_{,\psi}F_{\mu\lambda}F^{\lambda}_{\nu}, \tag{3}$$

where $K[\psi]_{,\psi} = \dfrac{\mathrm{d}K[\psi]}{\mathrm{d}\psi}$, and the corresponding generalized Maxwell equations are expressed in the following form:

$$\nabla_\mu(K_{,\psi}F^{\mu\nu}) = 0. \tag{4}$$

The spherically symmetric static metric is given by [65]

$$\mathrm{d}s^2 = -F(r)\mathrm{d}t^2 + \frac{1}{F(r)}\mathrm{d}r^2 + r^2\mathrm{d}\theta^2 + r^2\sin^2\theta\mathrm{d}\phi^2. \tag{5}$$

The only non-zero component of the Maxwell field tensor is $A_t = -\phi(r)$, and $\psi = -2\varphi'^2$. Next, we consider the specific expression $K[\psi] = -\psi - 2\Lambda + 2\sqrt{2}\alpha(-\psi)^{\frac{1}{2}}$, where α is a coupling constant and Λ is a cosmological constant factor. The corresponding solution to the field equations is given by [65]

$$\phi(r) = \frac{Q}{r} + r\alpha, \tag{6}$$

$$F(r) = 1 - \frac{2M}{r} + \frac{Q^2}{r^2} + \frac{r^2}{l^2} + 2\alpha Q - \frac{\alpha^2 r^2}{3}, \tag{7}$$

where Q, α, and l are the charge, coupling constant, and AdS radius, respectively. In the extended phase space, the cosmological constant is treated as the pressure, which is defined as $P = \dfrac{-\Lambda}{8\pi} = \dfrac{3}{8\pi l^2}$.

Using Eq. (7), the physical properties of the BH event horizon can be determined when $F(r) = 0$. Fig. 1 shows the behavior of the event horizon for different values of Q and α. It can be observed from Fig. 1(a) that the size of the BH increases with the increase in the charge Q. When $Q = 1.1$, a naked singularity appears, which means that no BH exists when Q exceeds the threshold. When Q is smaller than the threshold, two simple zeros appear, corresponding to two event horizons, as shown in Fig. 1(a) for $Q = 0.5, 0.7, 0.9$. It is clear from Fig. 1(b) that the size of the BH is also affected by the coupling constant α and increases as α increases.

The event horizon is located at $r = r_+$ and determined by $F(r) = 0$. M is the mass and can be expressed in terms of the horizon as

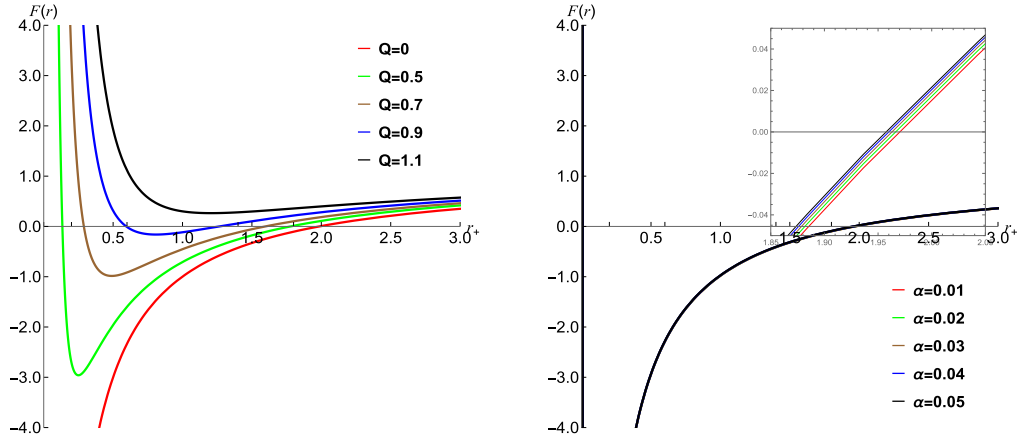

(a) $\alpha = 0.04$ and $M = 1$ (b) $Q = 0.12$ and $M = 1$

Fig. 1. (color online) Variation in $F(r)$ with respect to r of the NLED BH.

$$M = \frac{r_+}{2}\left(1 + \frac{Q^2}{r_+^2} + \frac{r_+^2}{l^2} + 2\alpha Q - \frac{\alpha^2 r_+^2}{3}\right). \tag{8}$$

When $\alpha = 0$, the metric is reduced to the RN AdS metric. When $\alpha = Q = 0$, the metric recovers to the Schwarzschild metric. The Hawking temperature and entropy are [67]

$$T = \frac{\kappa}{2\pi} = \frac{1}{4\pi}\left(\frac{1}{r_+} + \frac{3r_+}{l^2} - \frac{Q^2}{r_+^3} + \frac{2\alpha Q}{r_+} - \alpha^2 r_+\right), \tag{9}$$

$$S = \pi r_+^2. \tag{10}$$

The Gibbs free energy is

$$G = M - TS = \frac{1}{12 r_+}(9Q^2 + 3{r_+}^2 + 6\alpha Q {r_+}^2 + (\alpha^2 - \frac{3}{l^2}){r_+}^4). \tag{11}$$

Using Eq. (9), we can demonstrate that the horizon is a function of the temperature. When a specific temperature value is correlated with multiple values of the horizon radius, it serves as a clear indication that the BH experiences multiple distinct phases at that particular temperature. In contrast, when such a multi-valued correlation does not exist, it implies that no phase transition takes place within the BH. It is noteworthy that the critical temperature for this phase transition is determined by

$$\frac{\partial T}{\partial r_+} = 0, \quad \frac{\partial^2 T}{\partial r_+^2} = 0. \tag{12}$$

The critical curve in the coupling constant and charge $(Q - \alpha)$ space is shown in Fig. 2. The curve divides the plane into two distinct regions. Region A corresponds to the parameter range in which the BH undergoes an S/L phase transition, whereas in Region B, the BH remains in a stable single phase with no phase transition.

From the above equation, we obtain the analytical solution at the critical point:

$$r_{+c} = \sqrt{\frac{9l^2 - 3a^2l^4 + \sqrt{9a^2l^6 - 3a^4l^8}}{54 - 42a^2l^2 + 8a^4l^4}},$$
$$Q_c = \frac{a^2l^4 + \sqrt{9a^2l^6 - 3a^4l^8}}{2al^2(9 - 4a^2l^2)}, \tag{13}$$

and

$$T_c = \frac{(3 - a^2l^2)\sqrt{\dfrac{18l^2 - 6a^2l^4 + 2\sqrt{9a^2l^6 - 3a^4l^8}}{27 - 21a^2l^2 + 4a^4l^4}}}{3l^2\pi}. \tag{14}$$

We order $\alpha = 0.04$, $l = 1.00$, and obtain the values at the critical point as follows

$$r_{+c} = 0.411108, \quad Q_c = 0.168965, \quad T_c = 0.272423. \tag{15}$$

A graphical representation of the temperature as a function of the horizon radius is presented in Fig. 3. Each curve depicted in this figure corresponds to a distinct value of the charge of the BH. The figure reveals that no maximum values are present, which provides evidence that the BH exists in a single phase state under the condition of $Q > Q_c$. Conversely, when $Q < Q_c$, maximum values become evident in the plot. This phenomenon implies that the BH undergoes a transition to a multi phase state, with multiple distinct phases coexisting within its structure.

To study the phase transition further, we utilize Eqs. (9) and (11) to establish the relationship between the Gibbs free energy and temperature. The corresponding graphical representation is shown in Fig. 4. As clearly il-

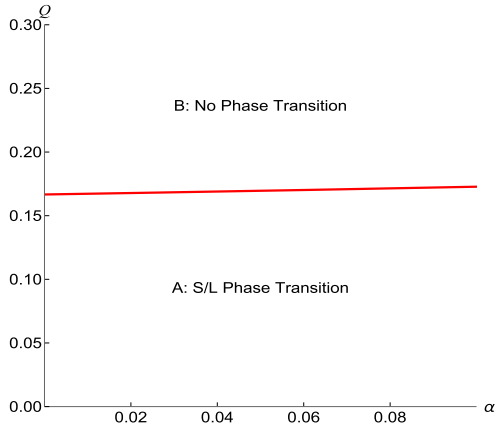

Fig. 2. (color online) Critical curve in the $Q-\alpha$ parameter space.

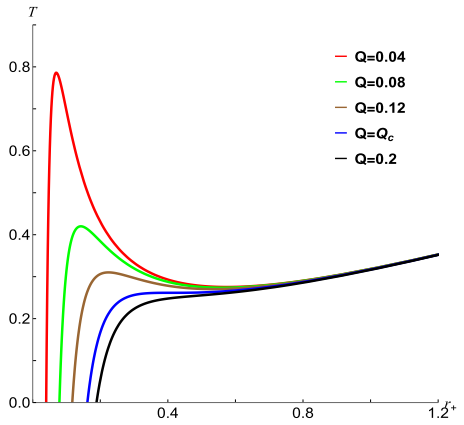

Fig. 3. (color online) Variation in the temperature with respect to the horizon radius of the NLED BH, where $\alpha = 0.04$.

lustrated in Fig. 4, when $Q < Q_c$, multiple phases emerge. These phases can be precisely categorized into three types: a small BH, intermediate BH, and large BH. It is of great significance to note that these three BH phases coexist within the temperature range $T_1 < T < T_2$. The temperature T_c marks the point where a first-order phase transition occurs. Conversely, when $Q > Q_c$, the BH system does not undergo any phase transition.

III. LEs AND PHASE TRANSITION OF NLED BH

In this section, we first obtain the LEs of chaos for the massless and charged particles in the equatorial plane around the four-dimensional NLED BH and then explore their relationships with the phase transition. Substantial work has focused on deriving the LEs. We first review the method developed in [57, 58].

A. LEs

When a particle with charge q moves in a circular orbit within the equatorial plane of the BH, its Lagrangian is

$$\mathcal{L} = \frac{1}{2}\left(-F\dot{t}^2 + \frac{\dot{r}^2}{F} + r^2\dot{\phi}^2\right) - qA_t\dot{t}, \tag{16}$$

where $\dot{x} = \dfrac{\mathrm{d}}{\mathrm{d}\tau}$ and τ is a proper time. From the Lagrangian, and using the definition of generalized momenta $\pi_\mu = \dfrac{\partial\mathcal{L}}{\partial\dot{x}}$, we obtain

$$\pi_t = \frac{\partial\mathcal{L}}{\partial\dot{t}} = -F\dot{t} - qA_t = -E, \quad \pi_r = \frac{\partial\mathcal{L}}{\partial\dot{r}} = \frac{\dot{r}}{F},$$
$$\pi_\phi = \frac{\partial\mathcal{L}}{\partial\dot{\phi}} = r^2\dot{\phi} = L. \tag{17}$$

In the above equation, E and L are the energy and angular momentum of the particle, respectively. Thus, the Hamiltonian is

$$H = \frac{1}{2F}(-(\pi_t + qA_t)^2 + \pi_r^2F^2 + \pi_\phi^2 r^{-2}F). \tag{18}$$

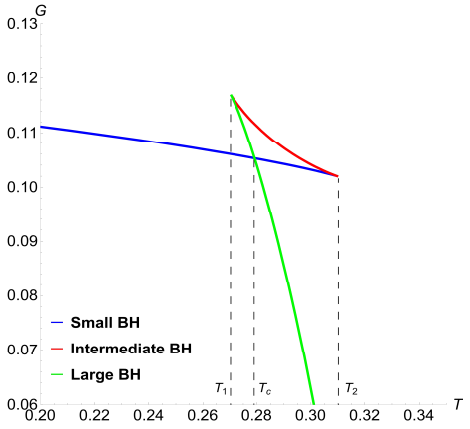

(a) $Q = 0.12 < Q_c$

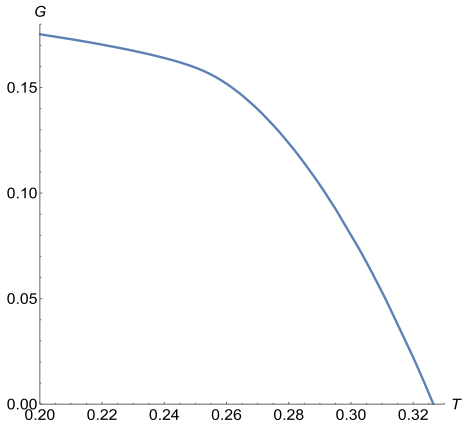

(b) $Q = 0.20 > Q_c$

Fig. 4. (color online) Variation in the Gibbs free energy with respect to the temperature of the NLED BH, where $\alpha = 0.04$.

From the Hamiltonian, the equations of motion are

$$\begin{aligned}
&\dot{t}=\frac{\partial H}{\partial \pi_t}=-\frac{\pi_t+qA_t}{F}, \quad \dot{\pi}_t=-\frac{\partial H}{\partial t}=0, \quad \dot{r}=\frac{\partial H}{\partial \pi_r}=\pi_r F,\\
&\dot{\pi}_r=-\frac{\partial H}{\partial r}=-\frac{1}{2}\left[\pi_r^2 F'-\frac{2qA_t'(\pi_t+qA_t)}{F}\right.\\
&\left.+\frac{(\pi_t+qA_t)^2F'}{F^2}-\pi_\phi^2(r^{-2})'\right],\\
&\dot{\phi}=\frac{\partial H}{\partial \pi_\phi}=\frac{\pi_\phi}{r^2}, \quad \dot{\pi}_\phi=-\frac{\partial H}{\partial \phi}=0.
\end{aligned} \tag{19}$$

In the above equations, the symbol "$\prime$" represents the derivative with respect to r. The normalization of the four-velocity of a particle is given by $g_{\mu\nu}\dot{x}^\mu\dot{x}^\nu=\eta$, where $\eta=0$ describes the case of a massless particle and $\eta=-1$ corresponds to the case of a massive particle. Using the normalization and the metric (5), we obtain a constraint condition for the charged particle,

$$\pi_t+qA_t=-\sqrt{F(1+\pi_r^2F+\pi_\phi^2r^{-2})}. \tag{20}$$

Using this constraint, we obtain the radial motion equations at time t,

$$\begin{aligned}
&\frac{\mathrm{d}r}{\mathrm{d}t}=\frac{\dot{r}}{\dot{t}}=-\frac{\pi_r F^2}{\pi_t+qA_t},\\
&\frac{\mathrm{d}\pi_r}{\mathrm{d}t}=\frac{\dot{\pi}_r}{\dot{t}}=-qA_t'+\frac{1}{2}\left[\frac{\pi_r^2FF'}{\pi_t+qA_t}+\frac{(\pi_t+qA_t)F'}{F}-\frac{\pi_\phi^2(r^{-2})'F}{\pi_t+qA_t}\right].
\end{aligned} \tag{21}$$

To calculate the LE, we select a phase space (r,π_r) and define a matrix with its elements given by

$$K_{11}=\frac{\partial F_1}{\partial r}, \quad K_{12}=\frac{\partial F_1}{\partial \pi_r}, \quad K_{21}=\frac{\partial F_2}{\partial r}, \quad K_{22}=\frac{\partial F_2}{\partial \pi_r}. \tag{22}$$

For convenience, we have defined $F_1=\frac{\mathrm{d}r}{\mathrm{d}t}$ and $F_2=\frac{\mathrm{d}\pi_r}{\mathrm{d}t}$. Considering the motion of the particle in an equilibrium orbit, we obtain $\pi_r=\frac{\mathrm{d}\pi_r}{\mathrm{d}t}=0$. From the constraint in Eq. (20), the matrix elements can be rewritten as [69]

$$\begin{aligned}
&K_{11}=\frac{\partial F_1}{\partial r}=0, \quad K_{22}=\frac{\partial F_2}{\partial \pi_r}=0,\\
&K_{12}=\frac{\partial F_1}{\partial \pi_r}=\frac{F^2}{\sqrt{F(1+\pi_\phi^2r^{-2})}},\\
&K_{21}=\frac{\partial F_2}{\partial_r}=-qA_t''-\frac{F''+\pi_\phi^2(r^{-2}F)''}{2\sqrt{F(1+\pi_\phi^2r^{-2})}}+\frac{\left[F'+\pi_\phi^2(r^{-2}F)'\right]^2}{4\left[F(1+\pi_\phi^2r^{-2})\right]^{3/2}}.
\end{aligned} \tag{23}$$

By calculating the eigenvalues of the above matrix, we obtain the LE at the specific radial position of the circular orbit, which takes the following form:

$$\begin{aligned}
\lambda^2=&\frac{1}{4}\left[\frac{F'+\pi_\phi^2(r^{-2}F)'}{1+\pi_\phi^2r^{-2}}\right]^2-\frac{1}{2}F\frac{F''+\pi_\phi^2(r^{-2}F)''}{1+\pi_\phi^2r^{-2}}\\
&-\frac{qA_t''F^2}{\sqrt{F(1+\pi_\phi^2r^{-2})}}.
\end{aligned} \tag{24}$$

It is clear that the exponent is affected by the angular momentum $\pi_\phi=L$, particle charge, and BH charge.

The charge of a massless particle is zero. The exponent of chaos for this particle is derived by following a procedure analogous to that described above, which is

$$\lambda^2=-\frac{1}{2}\frac{F(r^{-2}F)''}{r^{-2}}+\frac{1}{4}\frac{F\left[(r^{-2}F)'\right]^2}{F(r^{-2})^2}. \tag{25}$$

Obviously, it is not affected by the angular momentum at this time. Please refer to the Appendix for the derivation of the exponent for massless particles.

B. Case of massless particle

As demonstrated in [46–51], LEs exhibit a remarkable capability in revealing the thermodynamic phase transitions of BHs in AdS spacetimes. Building on this foundation, we first explore the correlation between the exponent of chaos for the massless particle and phase transition of the NLED BH, as illustrated in Fig. 5.

In this figure, when $Q>Q_c$, the exponent is single valued at all temperatures, indicating the absence of the phase transition. When $Q<Q_c$, the exponent is multivalued, and it approaches a constant value as the temperature increases. Specifically, Fig. 5(b) illustrates the temperature dependence of the exponent for $Q=0.12$. The exponent is single valued when $T<T_1$ and $T>T_2$, whereas it is multivalued when $T_1<T<T_2$. Within this temperature range $T<T<T_2$, two distinct scenarios emerge: For the small BH branch, the exponent increases slightly and then declines with an increasing temperature. For the large BH branch, the exponent decreases with an increasing temperature. In contrast, the intermediate BH branch exhibits an increase in the exponent as the temperature increases. By comparing Figs. 4 and 5, we observe that the temperature range with multivalued exponents corresponds precisely to the phase transition region shown in Fig. 4. Notably, for the large BH branch when $T>T_2$, as the temperature continues to increase, the exponent approaches 1.

For $Q>Q_c$, the exponent is single valued and approaches 1 as the temperature increases, as demonstrated in Fig. 5(c). A comparative analysis of Figs. 5(b) and (c) reveals that the multivalued nature of the exponent ex-

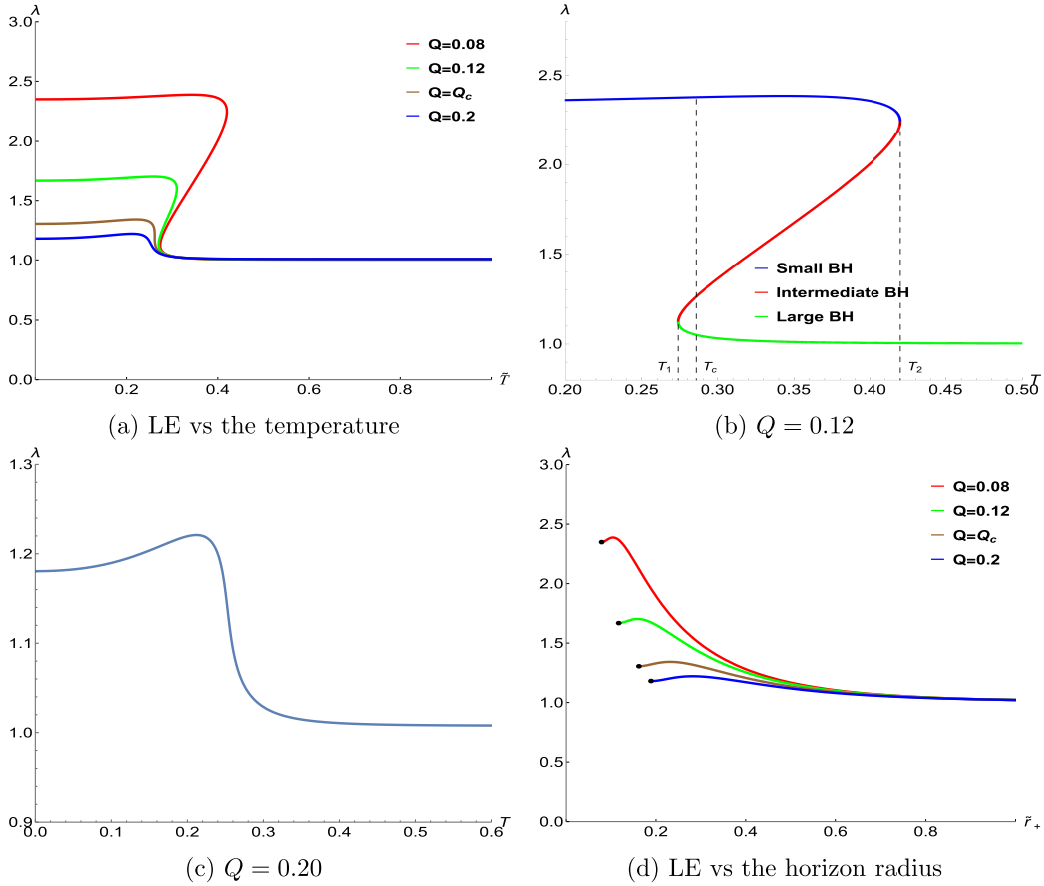

Fig. 5. (color online) Variation in the LE of chaos for the massless particle with respect to the temperature of the NLED BH.

clusively emerges when $Q < Q_c$, showing remarkable consistency with the free energy behavior observed in Fig. 4. To elucidate the correlation between the exponent and phase transition further, as well as to validate the completeness of our results, Fig. 5(d) presents a graph showing the functional relationship between the exponent and horizon radius. The black dots describe the case for $T = 0$. We observe that the exponent value decreases with an increasing charge at the extremal horizon (the horizon radius located at $T = 0$). Furthermore, as the horizon radius expands, all exponents approach 1, regardless of the values of the charge. This establishes that, for the massless particle, the LE serves as an effective probe for detecting the phase transition.

C. Case of charged particle

Throughout the calculations in this subsection, we fix $L = 20.00$ and $\alpha = 0.04$, and for a charged particle, we select $\eta = -1$ during the normalization of its four velocity. The position of its unstable orbit is determined by Eq. (21). By employing Eqs. (7) and (24), we derive the relationship between the exponent and temperature, which is plotted in Fig. 6. In this analysis, we set $q = 0.01$. The results presented in this figure exhibit similarities to those in Fig. 5. Specifically, when $Q < Q_c$, we observe distinct behaviors of the exponent of chaos for the charged particle around different sized BHs. The exponent for the case of small BHs initially increases slightly and then decreases as the temperature T increases, whereas the exponent for that of large BHs decreases monotonically with an increasing T. In contrast, for the case of intermediate BHs, the exponent increases with the temperature. However, when $Q > Q_c$, the exponent is single valued. Moreover, there exists a terminal temperature at which the exponent approaches zero, signifying the disappearance of the unstable orbit.

Figure 6(b) illustrates the scenario for $Q = 0.12$. When $T_1 < T < T_{p2}$, the exponent is a multivalued function of T, indicating the coexistence of large, intermediate, and samll BH phases within this temperature range. Concurrently, in the regime $T_{p2} < T < T_2$, the exponent also shows two distinct branches corresponding to the intermediate and small BH phases. At $T = T_{p2}$, the unstable orbit vanishes as the exponent approaches zero. Furthermore, Fig. 6(d) shows the functional relationship between the exponent and horizon radius. Through a comparative analysis of Fig. 6(b) and (d), we find the following: For small BHs, the exponent is significantly affected by the charge of the BH, decreasing with an increasing charge. For large BHs, the influence of the charge becomes negli-

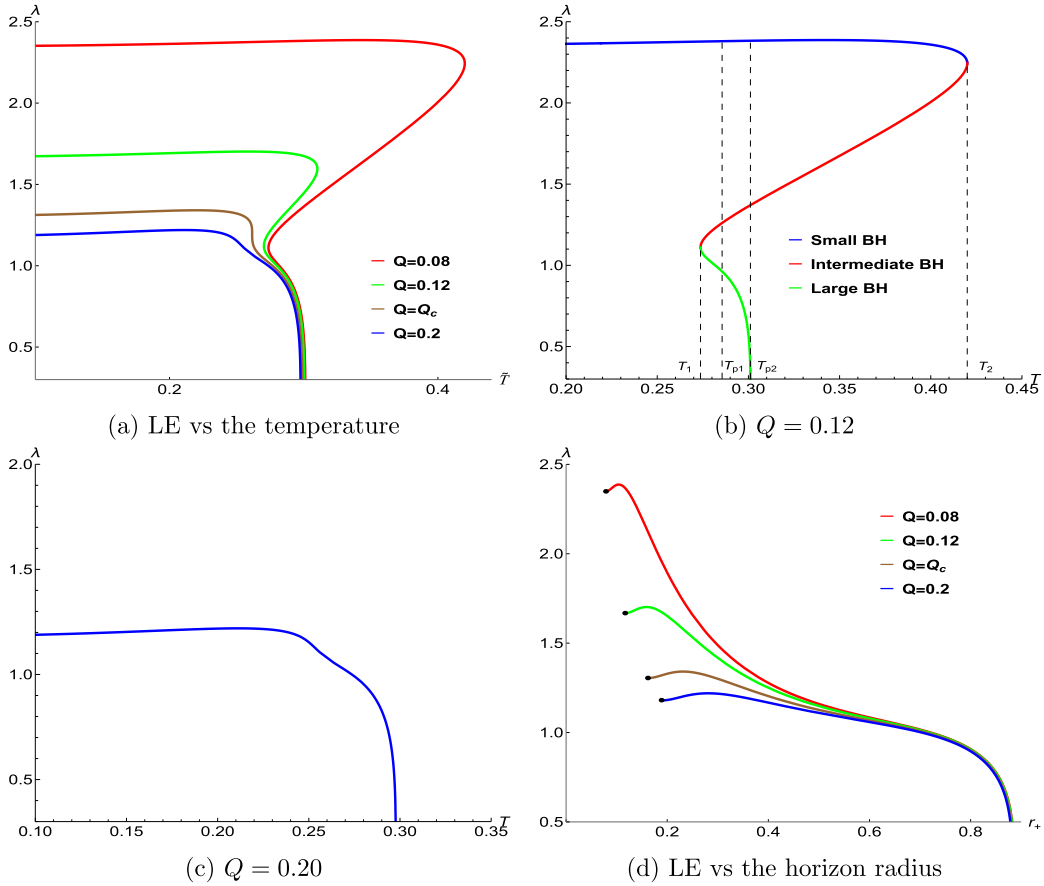

(a) LE vs the temperature (b) $Q = 0.12$

(c) $Q = 0.20$ (d) LE vs the horizon radius

Fig. 6. (color online) Variation in the LE of chaos for the charged particle with respect to the temperature of the NLED BH, where $q = 0.01$.

gible. All curves in Fig. 6(d) approach zero at almost identical critical radii, regardless of the values of the charge. This critical radius corresponds to the terminal temperature observed in Fig. 6(b). Therefore, the exponent for the charged particle also reveals the phase transition of the NLED BH.

The exponent of chaos for charged particles is also affected by the charge of the particle. Figure 7 depicts the relationship between the exponent and temperature for different values of the particle charge. For the sake of generality, we set $q = 0.01, 0.04, 0.07$, which is less than the charge of the BH. Upon analyzing Fig. 7, we observe two distinct effects of the charge on the system. First, although the overall influence of the charge on the exponent appears to be relatively minor in a broad sense, there is still a subtle yet discernible trend. Specifically, the exponent exhibits a slight decrease as the charge increases, but this change is well constrained within a certain limit. Second, the unstable orbital position of the particle undergoes variations with changes in the charge, which in turn leads to corresponding alterations in the exponent value. In conclusion, within the range where $q < Q$, the exponent remains a valid and reliable probe for detecting the phase transition in the NLED BH.

D. Crtical exponents

In this subsection, we calculate the critical exponents of the phase transition for the NLED BH to investigate the critical behavior of $\Delta\lambda$. The relationship between the critical exponent δ and $\Delta\lambda$ is defined as

$$\Delta\lambda \sim |T - T_C|^{\delta}, \tag{26}$$

where λ represents the chaos LE of particles. The horizon radius near the critical point can be written as

$$r_+ = r_i(1 + \epsilon). \tag{27}$$

Here, r_i is the horizon radius at the critical point and $|\epsilon \ll 1|$. The Hawking temperature T can be written as a function of r_+. $T(r_+)$ can be rewritten as

$$T(r_+) = T_i(1 + \xi), \tag{28}$$

where $|\xi \ll 1|$ and T_i is the critical temperature. Near the critical point, we perform a Taylor expansion of $T(r_+)$

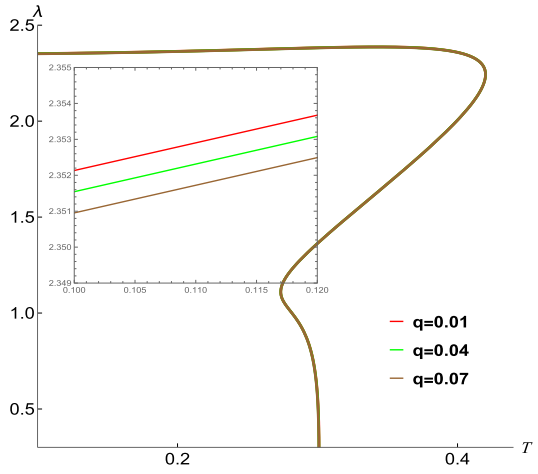

Fig. 7. (color online) Variation in the LE of chaos for different charged particles with respect to the temperature of the NLED BH.

and obtain the following equation:

$$T(r_+)=T(r_i)+\left(\frac{\partial T}{\partial r_+}\right)_c(r_+-r_i)+\frac{1}{2}\left(\frac{\partial^2 T}{\partial r_+^2}\right)_c(r_+-r_i)^2+O(r_i). \tag{29}$$

In the above equation, the subscript "c" denotes the value at the critical point. At the critical point, $\left(\frac{\partial T}{\partial r_+}\right)_c=0$, and thus, the second term on the right-hand side of the equation vanishes. Furthermore, neglecting the higher-order terms $O(r_i)$ and using Eqs. (27) and (29), we obtain

$$\epsilon^2=\frac{1}{2}\frac{T_i\xi}{r_i^2}\left(\frac{\partial^2 T}{\partial r_+^2}\right)_c. \tag{30}$$

Similarly, performing a Taylor expansion of $\lambda(r_+)$ in the vicinity of the critical point r_i yields

$$\lambda(r_+)=\lambda(r_i)+\left(\frac{\partial\lambda}{\partial r_+}\right)_c(r_+-r_i)+O(r_i). \tag{31}$$

Neglecting all higher-order terms in the above equation and using Eqs. (28), (30), and (31), we obtain

$$\lambda(r_+)-\lambda(r_i)=\left(\frac{\partial\lambda}{\partial r_+}\right)_c\left(\frac{1}{2}\frac{\partial^2 T}{\partial r_+^2}\right)^{-\frac{1}{2}}_{r_+=r_i}(T-T_i)^{\frac{1}{2}}. \tag{32}$$

The critical exponent δ is defined as $\Delta\lambda\sim|T-T_C|^{\delta}$. From the above equation, we observe that the critical exponent is $\delta=1/2$. In [47], $\Delta\lambda\equiv\lambda_L-\lambda_S$ is regarded as the order parameter, where λ_L and λ_S denote the LEs of the large/small BH phases. We obtain a result consistent with theirs, namely that the critical exponent is $\delta=1/2$.

IV. CHAOS BOUND

Maldacena, Shenker, and Stanford recently proposed that there exists a universal upper bound for the LE in thermal quantum systems with a large number of degrees of freedom [68],

$$\lambda\le\frac{2\pi T}{\hbar}, \tag{33}$$

where T represents the temperature of the system. Furthermore, within the context of single-particle systems, it has been further discovered that the upper bound of the exponent does not exceed the surface gravity of the BH [54]. However, recent studies have revealed that, for certain BHs within specific parameter ranges, the chaos bound is violated [53, 55, 56, 69–75]. When combined with the findings presented in the preceding sections, our results suggest that the exponent can serve as a reliable indicator of the BH phase transition. Consequently, we hypothesize the existence of an intrinsic connection between the chaos bound and the thermodynamic stability of BH. Specifically, our analysis indicates that the chaos bound may be violated during the phase transition, implying a potential link between chaotic dynamics and thermodynamic behavior in this system.

In Figs. 8 and 9, we elucidate the relationship between the LE and the surface gravity (κ normalized by $\frac{2\pi T}{\hbar}$) of the NLED BH, considering both the massless (Fig. 8) and charged (Fig. 9) particles. It is important to emphasize that r_2 in Figs. 8(a) and 9(a) denotes a critical radius at which the BH undergoes a phase transition from the small BH phase to the non-small BH phase, and this corresponds to the temperature T_2 depicted in Fig. 6(b). The left hand side of r_2 represents the stable branch of small BHs. $\lambda-\kappa>0$ indicates a violation of the chaos bound. Figure 8 illustrates the relationship between the LE characterized chaos for the massless particle and the horizon radius. As can be discerned from the figure, when the radius is less than r_2, a violation of the chaos bound occurs, indicating that the violation manifests in the spacetime of the stable small BH phase. Figure 8(b) depicts the scenario in which $Q=0.2>Q_c$. In this case, the NLED BH does not undergo a phase transition, yet we still observe a violation of the chaos bound. Moreover, by comparing it with Fig. 8(a), we find that an increase in the charge of the BH enlarges the threshold radius corresponding to the occurrence of the violation.

Figure 9 reveals the relationship between the LE characterized chaos for the charged particle and the horizon radius. In Fig. 9(a), as the angular momentum of the particle increases, the violation region of the chaos bound also expands. It is noteworthy that, similar to Fig. 8(a), the violation occurs solely in the spacetime of the stable small BH phase, and the violation region always remains

below the critical value r_2 at which the small BH phase transits to other phases. Figure 9(b) depicts the situation in which the BH does not experience a phase transition. We discover that an increase in the angular momentum also enlarges the region of the violation. Furthermore, by comparing it with Fig. 9(a), we find that an increase in the charge of the BH increases the threshold radius corresponding to the violation.

Figures 8 and 9 collectively demonstrate that violation of the chaos bound occurs regardless of whether the BH undergoes a phase transition. However, it is important to note that such a violation occurs only in the spacetime of small BHs with a thermodynamically stable phase.

V. CONCLUSIONS

We have studied the LEs of chaotic motion for both massless and charged particles orbiting around the NLED BH, and discussed their connections with the phase transition and chaos bound of this BH. The findings demonstrate that these exponents can effectively detect the phase transition.

In [76], the authors discovered that the violation of the chaos bound occurs within the stable phase of the BH. Our study further reveals that when a phase transition takes place, the violation occurs in the stable branch of the small BH. Moreover, the phenomenon of the violation manifests itself regardless of whether a phase transition occurs. Simultaneously, during the phase transition process, there exists a critical value for the horizon. Only when the horizon is smaller than this critical value does violation of the chaos bound occur. In addition, an increase in the angular momentum of the charged particle expands the region in which the chaos bound is violated.

A. Lyapunov exponent of massless particles

When a test particle moves in a circle around the

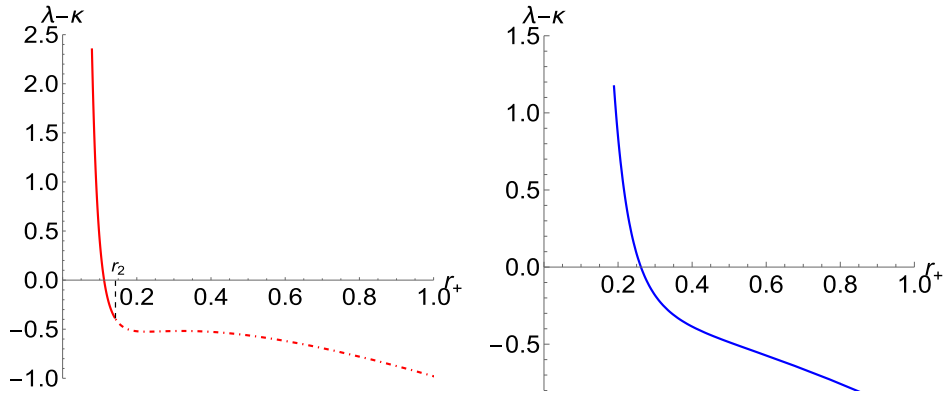

(a) $Q = 0.12$ (b) $Q = 0.20$

Fig. 8. (color online) Variation in the LE of chaos for the massless particle with respect to the horizon radius of the NLED BH. In (a), the solid line corresponds to the case of the small BH branch, whereas the dashed line corresponds to the case of the non-small (intermediate and large) BH branch.

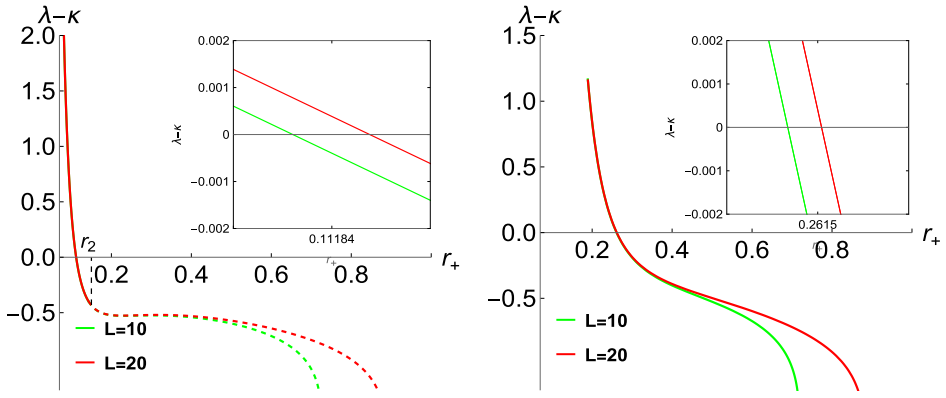

(a) $Q = 0.12$ (b) $Q = 0.20$

Fig. 9. (color online) Variation in the LE of chaos for the charged particle with respect to the horizon radius of the NLED BH. In (a), the solid line corresponds to the case of the small BH branch, whereas the dashed line corresponds to the case of the non-small (intermediate and large) BH branch.

equator of the black hole, the Lagrangian is

$$\mathcal{L} = \frac{1}{2}\left(-F\dot{t}^2 + \frac{\dot{r}^2}{F} + r^2\dot{\phi}^2\right), \tag{34}$$

Using $\pi_\mu = \frac{\partial \mathcal{L}}{\partial \dot{x}}$, we obtain the generalized momentum:

$$\begin{aligned} \pi_t &= \frac{\partial \mathcal{L}}{\partial \dot{t}} = -F\dot{t} = -E, \qquad \pi_r = \frac{\partial \mathcal{L}}{\partial \dot{r}} = \frac{\dot{r}}{F}, \\ \pi_\phi &= \frac{\partial \mathcal{L}}{\partial \dot{\phi}} = r^2\dot{\phi} = L. \end{aligned} \tag{35}$$

Here, E and L denote the energy and angular momentum of the particle, respectively. Thus, the Hamiltonian of the particle is

$$H = \frac{1}{2F}(-\pi_t^2 + \pi_r^2 F^2 + \pi_\phi^2 r^{-2} F). \tag{36}$$

From the Hamiltonian, the motion equations of the particle are obtained, as follows:

$$\begin{aligned} \dot{t} &= \frac{\partial H}{\partial \pi_t} = -\frac{\pi_t}{F}, \quad \dot{\pi}_t = -\frac{\partial H}{\partial t} = 0, \quad \dot{r} = \frac{\partial H}{\partial \pi_r} = \pi_r F, \\ \dot{\pi}_r &= -\frac{\partial H}{\partial r} = -\frac{1}{2}\left[\pi_r^2 F' + \frac{\pi_t^2 F'}{F^2} - \pi_\phi^2 r^{-4}(r^2)'\right], \\ \dot{\phi} &= \frac{\partial H}{\partial \pi_\phi} = \frac{\pi_\phi}{r^2}, \quad \dot{\pi}_\phi = -\frac{\partial H}{\partial \phi} = 0. \end{aligned} \tag{37}$$

Here, we again apply the normalization condition of the four-velocity of. theparticle, where $\eta = 0$ corresponds to the case of massless particles, yielding the constraint condition.

$$\pi_t = -\sqrt{F(\pi_r^2 N + \pi_\phi^2 r^{-2})}. \tag{38}$$

Similarly, we derive the relationship between the radial coordinate and time for the massless particle.

$$\begin{aligned} \frac{\mathrm{d}r}{\mathrm{d}t} &= \frac{\dot{r}}{\dot{t}} = -\frac{\pi_r F^2}{\pi_t}, \\ \frac{\mathrm{d}\pi_r}{\mathrm{d}t} &= \frac{\dot{\pi}_r}{\dot{t}} = \frac{1}{2}\left[\frac{\pi_r^2 F F'}{\pi_t} + \frac{\pi_t F'}{F} - \frac{\pi_\phi^2 r^{-4}(r^2)' F}{\pi_t}\right]. \end{aligned} \tag{39}$$

For the massless particle, Eq. (39) is reformulated using the constraint in Eq. (38) and becomes

$$\begin{aligned} F_1 &= \frac{\pi_r F^2}{\sqrt{F(\pi_r^2 F + \pi_\phi^2 r^{-2})}}, \\ F_2 &= -\frac{\pi_r^2 (F^2)'}{2\sqrt{F(\pi_r^2 F + \pi_\phi^2 r^{-2})}} - \frac{\pi_\phi^2 (r^{-2}F)'}{2\sqrt{F(\pi_r^2 F + \pi_\phi^2 r^{-2})}}. \end{aligned} \tag{40}$$

Considering the circular motion of the particle, its constraint condition satisfies

$$\pi_r = \frac{\mathrm{d}\pi_r}{\mathrm{d}t} = 0. \tag{41}$$

For a massless particle, when $\eta = 0$, it naturally reduces to the photon sphere case, and we determine its orbit based on $F_2 = 0$. Using Eqs. (22) and (40), we derive the Jacobian matrix in phase space (r, π_r) and compute its eigenvalues to obtain the Lyapunov exponent. The elements of the Jacobian matrix are as follows:

$$\begin{aligned} K_{11} &= \frac{\partial F_1}{\partial r} = 0, \\ K_{12} &= \frac{\partial F_1}{\partial \pi_r} = \frac{F^2}{\sqrt{F(\pi_\phi^2 r^{-2})}}, \\ K_{21} &= \frac{\partial F_2}{\partial_r} = -\frac{\pi_\phi^2 (r^{-2}F)''}{2\sqrt{F(\pi_\phi^2 r^{-2})}} + \frac{\left[\pi_\phi^2 (r^{-2}F)'\right]^2}{4\left[F(\pi_\phi^2 r^{-2})\right]^{3/2}}, \\ K_{22} &= \frac{\partial F_2}{\partial \pi_r} = 0. \end{aligned} \tag{42}$$

The chaos exponent of the massless particle can be obtained by calculating the eigenvalues of the matrix, as follows:

$$\lambda^2 = -\frac{1}{2}\frac{F(r^{-2}F)''}{r^{-2}} + \frac{1}{4}\frac{F\left[(r^{-2}F)'\right]^2}{F(r^{-2})^2}. \tag{43}$$

ACKNOWLEDGMENTS

We sincerely thank the reviewers for their valuable comments and constructive suggestions, which have greatly improved this work.

References

[1] S.W. Hawking and D. N. Page, Commun. Math. Phys. **87**, 577 (1983)
[2] D. Kastor, S. Ray, and J. Traschen, Class. Quant. Grav. **26**, 195011 (2009)
[3] D. Kastor, S. Ray, and J. Traschen, Class. Quant. Grav. **27**, 235014 (2010)
[4] D. Kubiznak and R. B. Mann, JHEP **07**, 033 (2012)
[5] R. G. Cai, L. M. Cao, L. Li *et al.*, JHEP **09**, 005 (2013)
[6] S. W. Wei and Y. X. Liu, Phys. Rev. Lett **115**, 111302 (2015)
[7] S. W. Wei, Y. X. Liu, and R. B. Mann, Phys. Rev. Lett **123**,

071103 (2019)
[8] S. W. Wei and Y. X. Liu, Phys. Rev. D **87**, 044104 (2013)
[9] S.W. Wei and Y. X. Liu, Phys. Rev. D **90**, 044057 (2014)
[10] S. Gunasekaran, R. B. Mann, and D. Kubiznak, JHEP **11**, 110 (2012)
[11] W. Xu and L. Zhao, Phys. Lett. B **736**, 214 (2014)
[12] A. M. Frassino, D. Kubiznak, R. B. Mann *et al*., JHEP **09**, 080 (2014)
[13] N. Altamirano, D. Kubiznak, and R. B. Mann, Phys. Rev. D **88**, 101502 (2013)
[14] N. Altamirano, D. Kubiznak, R. B. Mann *et al*., Class. Quant. Grav. **31**, 042001 (2014)
[15] M. H. Dehghani, S. Kamrani, and A. Sheykhi, Phys. Rev. D **90**, 104020 (2014)
[16] B. P. Dolan, A. Kostouki, D. Kubiznak *et al*., Class. Quant. Grav. **31**, 242001 (2014)
[17] E. Caceres, P. H. Nguyen, and J. F. Pedraza, JHEP **09**, 184 (2015)
[18] S. Chakraborty and T. Padmanabhan, Phys. Rev. D **92**, 104011 (2015)
[19] R. A. Hennigar, R. B. Mann and E. Tjoa, Phys. Rev. Lett. **118**, 021301 (2017)
[20] D. Momeni, M. Faizal, K. Myrzakulov *et al*., Phys. Lett. B **765**, 154 (2017)
[21] J. P. S. Lemos and O. B. Zaslavskii, Phys. Lett. B **786**, 296 (2018)
[22] J. F. Pedraza, W. Sybesma and M. R. Visser, Class. Quant. Grav. **36**, 054002 (2019)
[23] P. Wang, H. Wu, and H. Yang, JCAP **04**, 052 (2019)
[24] M. Zhang, S. Z. Han, J. Jiang *et al*., Phys. Rev. D **99**, 065016 (2019)
[25] S. W. Wei and Y. X. Liu, Phys. Rev. D **97**, 104027 (2018)
[26] S. W. Wei, Y. X. Liu, and Y. Q. Wang, Phys. Rev. D **99**, 044013 (2019)
[27] M. Zhang and M. Guo, Eur. Phys. J. C **80**, 790 (2020)
[28] A. Belhaj, L. Chakhchi, H. El Moumni *et al*., Int. J. Mod. Phys. A **35**, 2050170 (2020)
[29] Y. Liu, D. C. Zou and B. Wang, JHEP **09**, 179 (2014)
[30] S. Mahapatra, JHEP **04**, 142 (2016)
[31] M. Chabab, H. El Moumni, S. Iraoui *et al*., Eur. Phys. J. C **76**, 676 (2016)
[32] M. Zhang, C. M. Zhang, D. C. Zou *et al*., Chin. Phys. C **45**, 045105 (2021)
[33] Y. Sota, S. Suzuki, and K. i. Maeda, Class. Quant. Grav. **13**, 1241 (1996)
[34] N. Kan and B. Gwak, Phys. Rev. D **105**, 026006 (2022)
[35] B. Gwak, N. Kan, B. H. Lee *et al*., JHEP **09**, 026 (2022)
[36] W. Hanan and E. Radu, Mod. Phys. Lett. A **22**, 399 (2007)
[37] J. R. Gair, C. Li, and I. Mandel, Phys. Rev. D **77**, 024035 (2008)
[38] A. M. Al Zahrani, V. P. Frolov, and A. A. Shoom, Phys. Rev. D **87**, 084043 (2013)
[39] L. Polcar and O. Semerak, Phys. Rev. D **100**, 103013 (2019)
[40] M. Wang, S. Chen, and J. Jing, Eur. Phys. J. C **77**, 208 (2017)
[41] S. Chen, M. Wang and J. Jing, JHEP **09**, 082 (2016)
[42] F. Lu, J. Tao, and P. Wang, JCAP **12**, 036 (2018)
[43] K. Li, D. Z. Ma, and Z. M. Xu, Phys. Lett. B **860**, 139164 (2025)
[44] V. Cardoso, A. S. Miranda, E. Beri *et al*., Phys. Rev. D **79**, 064016 (2009)
[45] X. Guo, Y. Lu, B. Mu *et al*., JHEP **08**, 153 (2022)
[46] S. J. Yang, J. Tao, B. R. Mu *et al*., JCAP **07**, 045 (2023)
[47] X. Lyu, J. Tao, and P. Wang, Eur. Phys. J. C **84**, 974 (2024)
[48] A. N. Kumara, S. Punacha, and M. S. Ali, JCAP **07**, 061 (2024)
[49] Y. Z. Du, H. F. Li, L. B. Ma *et al*., arXiv: 2403.20083
[50] B. Shukla, P. P. Das, D. Dudal *et al*., Phys. Rev. D **110**, 024068 (2024)
[51] N. J. Gogoi, S. Acharjee, and P. Phukon, Eur. Phys. J. C **84**, 1144 (2024)
[52] Y. Z. Du, H. F. Li, Y. B. Ma *et al*., Eur. Phys. J. C **85**, 1 (2025)
[53] N. Kan and B. Gwak, Phys. Rev. D **105**, 026006 (2022)
[54] K. Hashimoto and N. Tanahashi, Phys. Rev. D **95**, 024007 (2017)
[55] Q. Q. Zhao, Y. Z. Li, and H. Lu, Phys. Rev. D **98**, 124001 (2018)
[56] B. Gwak, N. Kan, B. H. Lee *et al*., JHEP **09**, 026 (2022)
[57] Y. Q. Lei, X. H. Ge, and C. Ran, Phys. Rev. D **104**, 046020 (2021)
[58] Y. Q. Lei and X. H. Ge, Phys. Rev. D **105**, 084011 (2022)
[59] C. S. Camara, M. R. de Garcia Maia, J. C. Carvalho *et al*., Phys. Rev. D **69**, 123504 (2004)
[60] E. Elizalde, J. E. Lidsey, S. Nojiri *et al*., Phys, Lett. B **574**, 1 (2003)
[61] J. M. Bardeen, in *Conference Proceedings of GR5* (Tbilisi: URSS, 1968), p. 174
[62] K.A. Bronnikov, Phys. Rev. D **63**, 044005 (2001)
[63] S.A. Hayward, Phys. Rev. Lett **96**, 031103 (2006)
[64] L. Balart and E. C. Vagenas, Phys. Rev. D **90**, 124045 (2014)
[65] S. Yu and C. J. Gao, Int. J. Mod. Phys. D **29**, 2050032 (2020)
[66] Z. Y. Fan and X. Wang, Phys. Rev. D **94**, 124027 (2016)
[67] A. Jawad, S. Chaudhary, and K. Jusufi, Eur. Phys. J. C **82**, 655 (2022)
[68] J. Maldacena, S. H. Shenker, and D. Stanford, JHEP **08**, 106 (2016)
[69] C. H. Gao, D. Y. Chen, C. Y. Yu *et al*., Phys. Lett. B **833**, 137343 (2022)
[70] D. Y. Chen and C. H. Gao, New J. Phys. **24**, 123014 (2022)
[71] S. Dalui, B. R. Majhi, and P. Mishra, Phys. Lett. B **788**, 486 (2019)
[72] S. Dalui, B. R. Majhi, and P. Mishra, Int. J. Mod. Phys. A **35**, 2050081 (2020)
[73] J. Park and B. Gwak, JHEP **04**, 023 (2024)
[74] S. Jeong, B. H. Lee, and W. Lee, Phys. Rev. D **107**, 104037 (2023)
[75] J. Xie, J. Wang, and B. Tang, Phys. Dark. Univ **42**, 101271 (2023)
[76] Y. Q. Lei, X. H. Ge, and S. Dalui, Phys. Lett. B **856**, 138929 (2024)